energies

MDPI

Article

Continuous-Flow Ultrasonic-Assisted Plasma-Driven Solution Electrolysis Reactors for Crude Oil Degradation in Hypersaline Produced Water with Hydrogen Co-Production

Sergii Bespalko [1,*], Oleksii Halychyi [1], Justyna Markiewicz [1], Najah M. Al Mhanna [2,3], Marcin Siedlecki [1] and Jerzy Mizeraczyk [4]

[1] Research and Innovation Centre Pro-Akademia, Innowacyjna Street 9/11, 95-050 Konstantynów Łódzki, Poland
[2] Department of Engineering, German University of Technology in Oman, Muscat 1816, Oman
[3] Oman Hydrogen Center, German University of Technology in Oman, Muscat 1816, Oman
[4] Department of Power Electronics, Gdynia Maritime University, Morska Street 83, 81-225 Gdynia, Poland
* Correspondence: sergii.bespalko@proakademia.eu

Abstract

This work evaluates the performance of three configurations (V1, V2, and V3) of novel membraneless continuous-flow ultrasonic-assisted plasma-driven solution electrolysis (PDSE) reactors (*CombiSonoPlasma*®) operated at near-ambient temperature and pressure, for the single-pass treatment of model hypersaline produced water (HPW) originating from the oil extraction industry, with simultaneous hydrogen co-production. The performance of the reactors was assessed based on (i) the formation of gaseous oil decomposition products (CO, CO_2, and CH_4) as indicators of crude oil destruction and (ii) hydrogen generation as a valuable energy co-product. The results demonstrate that coupling ultrasonication with PDSE provides a bidirectional synergistic effect: ultrasonication reduces the PDSE electric power demand, while PDSE operation simultaneously decreases the power consumption of the ultrasonic generator. Among the investigated configurations, along with improved oil decomposition, Reactor V2 delivered the most pronounced energy benefits, achieving reductions in electrical power consumption of 33.5% for PDSE and 44.5% for the ultrasonic generator. These findings highlight the potential of continuous-flow ultrasound-assisted PDSE as an energy-efficient process intensification strategy for oilfield HPW treatment combined with hydrogen co-generation.

Keywords: advanced oxidation process (AOP); hypersaline produced water (HPW); crude oil degradation; plasma-driven solution electrolysis (PDSE); sonolysis; hydrogen co-production; process intensification; energy efficiency; continuous-flow PDSE reactor

Check for updates

Academic Editor: Antonio Zuorro

Received: 12 June 2026
Revised: 7 July 2026
Accepted: 16 July 2026
Published: 22 July 2026

Correction Statement: This article has been republished with a minor change. The change does not affect the scientific content of the article and further details are available within the backmatter of the website version of this article.

Copyright: © 2026 by the authors. Licensee MDPI, Basel, Switzerland. This article is an open access article distributed under the terms and conditions of the Creative Commons Attribution (CC BY) license.

1. Introduction

The plasma-driven solution electrolysis (PDSE), also known as plasma electrolysis or contact glow discharge electrolysis (CGDE), has recently attracted considerable attention as an advanced oxidation process (AOP) demonstrating outstanding efficiency in the treatment of industrial, agricultural, and domestic wastewater containing harmful pollutants such as aromatic compounds, dyes, organic solvents, surfactants, pesticides, and pathogenic microorganisms [1,2]. The high treatment efficiency of PDSE is attributed to the formation of extreme physicochemical conditions in the vicinity of the discharge electrode, where pollutants are affected by: (i) high temperatures exceeding 3000 K in the plasma zone

surrounding the discharge electrode [3], enabling complete degradation of organic and inorganic pollutants; (ii) ultraviolet (UV) radiation emitted by the plasma; and (iii) highly reactive oxidizing species, in particular hydroxyl radicals ($OH^{\bullet}$), which possess one of the highest oxidation potentials among known oxidants [4], as well as hydrogen peroxide (H_2O_2), an environmentally friendly oxidant [5] generated in high local concentrations within the liquid-phase reaction zone surrounding the plasma.

In addition to wastewater treatment, plasma–liquid interactions in PDSE have demonstrated efficient hydrogen production through simultaneous electrochemical and plasma-chemical reaction pathways, particularly in aqueous electrolyte solutions containing high concentrations of organic compounds, especially alcohols [6]. Furthermore, the recent comprehensive analysis by Bespalko and Mizeraczyk [6] highlighted the superiority of PDSE over other plasma-assisted methods for hydrogen production from water–organic mixtures in terms of both hydrogen production rate [$g(H_2)/h$] and energy yield [$g(H_2)/kWh$].

Ultrasound has also been extensively investigated as an AOP technique for wastewater treatment [7], as well as an alternative route for green hydrogen production [8]. When ultrasonic waves propagate through a liquid, acoustic cavitation occurs. This phenomenon involves bubble nucleation, growth, collapse, and implosion. During bubble implosion, extreme local temperatures (approximately 5000 K) and pressures (approximately 2000 bar) are generated due to rapid adiabatic compression of the gas–vapor mixture inside the bubbles. Under certain conditions, the pressure within transient cavitation bubbles may reach up to 10,000 bar. These conditions strongly depend on cavitation dynamics, which are influenced by factors such as liquid properties, initial bubble size, and acoustic field intensity. Consequently, large amounts of highly reactive hydrogen ($H^{\bullet}$) and hydroxyl radicals ($OH^{\bullet}$) are generated within the cavitation zone. Through this mechanism, the application of high-frequency ultrasonic waves to water, commonly referred to as *sonolysis*, represents a viable approach to green hydrogen production [9].

Recently, experiments involving indirect ultrasonication at 40 kHz to assist cathodic PDSE demonstrated a positive effect, reducing the electric power required to sustain plasma discharges by 21.5% compared with cathodic PDSE without ultrasonication [10]. In indirect ultrasonication, ultrasonic energy is transmitted through an intermediate liquid medium (e.g., water in an ultrasonic bath) to the treated solution without direct contact between the ultrasonic source and the sample. Although this approach demonstrated promising synergistic effects, part of the ultrasonic energy is inevitably dissipated during transmission through the intermediate medium and reactor walls.

To enhance the efficiency of acoustic energy transfer and intensify cavitation effects directly within the reaction zone, three continuous-flow reactor configurations were designed in the present research to enable direct ultrasonication of cathodic PDSE. In direct ultrasonication, the ultrasonic horn (sonotrode) is immersed directly into the treated solution, allowing high-intensity ultrasonic energy to be delivered directly to the plasma–liquid interaction region. The performance of these three continuous-flow, direct ultrasonic-assisted PDSE reactors was evaluated for the treatment of model hypersaline produced water (HPW) with concurrent hydrogen production.

2. Research Gap and Significance of the Proposed Continuous-Flow Ultrasonic-Assisted PDSE Strategy

Despite the considerable progress achieved in plasma-driven solution electrolysis (PDSE) and ultrasound-assisted advanced oxidation processes (AOPs), several important limitations still hinder their practical implementation for industrial wastewater treatment. Conventional PDSE reactors are predominantly operated in batch mode [2] and generally require relatively high electrical power to initiate and sustain plasma discharges. Fur-

thermore, their performance is often constrained by limited mass transfer between the plasma–liquid interface and the bulk solution, insufficient mixing, and a relatively short residence time of pollutants within the active reaction zone [6]. Likewise, although ultrasonic cavitation has been widely recognized as an effective AOP for wastewater treatment and hydrogen production [7–9], its stand-alone application is frequently associated with considerable energy consumption and relatively low energy efficiency, limiting its large-scale industrial implementation [11]. Recent reviews have therefore emphasized that further process intensification and hybridization strategies are required to improve the energy efficiency and practical applicability of plasma- and ultrasound-based technologies [12–14].

Furthermore, previous studies on ultrasound-assisted PDSE have primarily focused on indirect ultrasonication, in which ultrasonic waves are transmitted through an intermediate liquid medium and the reactor walls before reaching the plasma region [10]. Such an arrangement inevitably dissipates part of the acoustic energy, reducing cavitation intensity within the plasma–liquid interaction zone and limiting the achievable synergistic effects. Consequently, there remains a need for reactor concepts capable of simultaneously enhancing pollutant degradation, improving hydrogen production, reducing the energy demand of both technologies, and enabling continuous-flow operation suitable for future industrial implementation. Recent studies on ultrasound-assisted electrolysis have shown that direct acoustic coupling substantially improves gas bubble detachment, enhances mass transfer, and reduces electrochemical overpotentials, highlighting the advantages of direct ultrasonic energy delivery to the reaction zone [13,14].

The continuous-flow direct ultrasonic-assisted PDSE strategy proposed in this work addresses these challenges by integrating direct ultrasonication with plasma-driven solution electrolysis in a single membraneless reactor. Direct immersion of the sonotrode into the cathodic compartment enables acoustic energy to be delivered directly into the plasma region, thereby intensifying cavitation, improving hydrodynamics and mass transfer, accelerating gas bubble removal from the discharge region, and enhancing interactions between plasma-generated reactive species and organic pollutants. In addition, the continuous-flow reactor configuration enables single-pass wastewater treatment, representing an important step toward industrial process scale-up. Similar benefits of ultrasound-assisted electrochemical processes, including enhanced bubble dynamics, improved mass transfer, lower electrical resistance, and increased hydrogen production efficiency, have recently been reported in the literature [13–15].

The significance of the proposed strategy extends beyond the development of a new reactor configuration. To the best of our knowledge, this study demonstrates for the first time a bidirectional synergistic interaction between ultrasonication and plasma-driven solution electrolysis. In addition to confirming that ultrasonication decreases the electrical power required to sustain plasma discharges, the present work also reveals the previously unreported reverse phenomenon whereby stable PDSE operation reduces the electrical power consumption of the ultrasonic generator. Moreover, the optimized reactor configuration promotes crude oil retention within the plasma treatment zone, enhances hydrogen co-production, and improves the overall energy efficiency of hypersaline produced water treatment. These findings demonstrate that the proposed *CombiSonoPlasma*® concept represents a promising process intensification strategy for simultaneous wastewater treatment and renewable hydrogen generation, while contributing to the development of next-generation hybrid plasma-cavitation reactors for industrial water treatment applications [12–14].

3. Materials and Methods

3.1. Description of the Experimental Setup and Procedure

The three continuous-flow direct ultrasonic-assisted PDSE reactors were designed for the treatment of model HPW, formulated to replicate the composition and crude oil contamination level of actual HPW. Schematic representations of the reactors, designated as V1, V2, and V3, are shown in Figure 1.

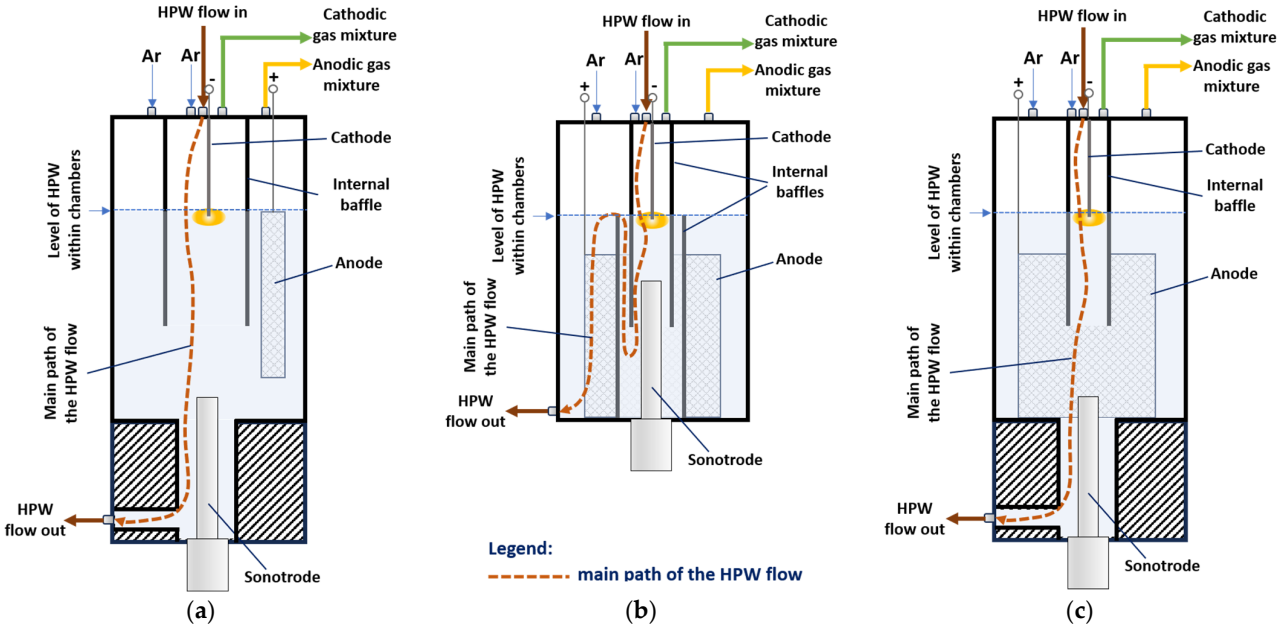


Figure 1. Schemes of the designed and studied ultrasonic-assisted PDSE reactors: (**a**) reactor V1, (**b**) reactor V2, (**c**) reactor V3. The brown dashed line is the main path of the HPW flow. The reactor design is the subject of a patent application No. P.451120 [WIPO ST 10/C PL451120], filed in 2025.

Below is a brief description of the operating principle of the ultrasonic-assisted PDSE reactors. Each reactor contained two electrodes of different polarity and geometry: an anode and a cathode. The anode was fully immersed in the model HPW, whereas only 5 mm of the cathode tip was submerged. Owing to the substantially smaller active surface area of the cathode relative to the anode, plasma formation during DC electrolysis was initiated at the cathode as the applied voltage increased. In all reactor configurations, the discharge electrodes consisted of tungsten rods with a diameter of 2 mm. The working volume of each reactor was 2 L.

To minimize mixing of anodic and cathodic gaseous products, the internal space within each reactor above the HPW level was divided into two separate compartments by a baffle arrangement. During operation, both compartments were continuously purged with argon at a flow rate of 348 sccm. Continuous supply and discharge of the model HPW were realized through the top and bottom of the reactors, respectively, as illustrated in Figure 1. First, the model HPW entered the cathodic chamber from the top, then flowed to the anodic chamber and then to the outlet at the reactor's bottom. The plasma generated at the cathode caused the decomposition of organic contaminants present in the model HPW while simultaneously producing hydrogen in the cathodic compartment.

In addition to PDSE, ultrasonic irradiation was introduced into the cathodic chamber through a cylindrical ultrasonic horn (sonotrode) positioned beneath the discharge electrode at the bottom of the reactor, as shown in Figure 1. Direct sonication of the plasma region enhanced mixing of the model HPW and promoted the release of the gaseous products through a degassing effect, primarily by stimulating the coalescence of microbubbles within

the liquid phase [10]. The ultrasonic irradiation at a frequency of 20 kHz was generated using a Sonopuls HD 4400 ultrasonic system (BANDELIN electronic GmbH & Co. KG, Berlin, Germany).

The following key differences distinguished reactor configurations V1, V2, and V3:

1. Different counter-electrode geometries were investigated. In reactor V1, the anode consisted of a flat Pt-coated titanium mesh plate (30 mm × 70 mm with a thickness of 1 mm). In contrast, reactors V2 and V3 employed cylindrical Pt-coated titanium mesh anodes with an internal diameter of 97 mm, a height of 100 mm, and a thickness of 1 mm, providing an anodic active surface area substantially larger than that of the cathode.
2. The internal diameter of the cathodic compartment in reactor V1 was considerably larger than that of reactors V2 and V3 (74 mm in reactor V1 versus 35 mm in reactors V2 and V3).
3. Reactor V2 was equipped with an additional baffle installed at the bottom of the reactor, creating a labyrinth-type coaxial flow path for the model HPW (Figure 1b) as it moved from the cathodic compartment to the anodic compartment. Such a design was intended to increase the retention time of the model HPW within the ultrasonic-assisted PDSE reactor.
4. Unlike reactors V1 and V3, reactor V2 featured a sonotrode installed deeper into the cathodic compartment, enabling more intensive treatment of the flowing model HPW.

The following process parameters were monitored during the experiments:

- Electrical current and voltage between the cathode and anode;
- Pressure and temperature of the model HPW in the cathodic and anodic compartments;
- Temperature of the cathodic gas mixture evolved from the cathodic compartment;
- Flow rate of the cathodic gas mixture;
- Total organic carbon (TOC) values of the treated HPW;
- Volume concentrations of hydrogen, oxygen, carbon monoxide, carbon dioxide, and methane in the cathodic gas mixture;
- Mass loss of the discharge electrode.

The experimental setup used for these measurements is shown in Figure 2. A detailed description can be found in [16].

The influent model HPW was prepared to have the following composition (Chempur, Piekary Śląskie, Poland): NaCl (7.497 wt%), $MgCl_2 \cdot 6H_2O$ (1.770 wt%), $CaCl_2 \cdot 6H_2O$ (4.166 wt%), $NaHCO_3$ (0.040 wt%), and Na_2SO_4 (0.013 wt%), using an AS220.3Y analytical balance (RADWAG Wagi Elektroniczne, Radom, Poland). To simulate oil contamination, crude oil was added at an initial concentration of 400 mg/L (Protolab, Słupsk, Poland). Continuous circulation was maintained using two Aqua-Trend peristaltic pumps (Aqua-Trend Łukasz Pawłowski, Łódź, Poland) operating at a flow rate of 0.5 L/min. Prior to reactor operation, the initial temperature of the model HPW was 23.2 °C.

The electrical power supply used for plasma generation consisted of an LTC-300-8D variable autotransformer (RUCELF Co., Ltd., Kolomna, Russia) integrated with a diode rectifier bridge and two 16 mF smoothing capacitors (KEMET Electronics Corporation, Simpsonville, SC, USA). The voltage applied between the electrodes was measured using a P20H voltage transducer (LUMEL S.A., Zielona Góra, Poland) with an operating range of −400 to +400 V DC, while the current was measured using an AC-11 DC current sensor (F&F Filipowski sp. j., Pabianice, Poland) rated for 20 A. Gas pressures in the cathodic and anodic compartments were measured using DMP331 pressure sensors (BD SENSORS GmbH, Thierstein, Germany). Electrolyte temperatures in both chambers, together with the outlet cathodic gas temperature, were monitored using TOPE-361 Pt100 resistance

temperature detectors (LIMATHERM Sensor Sp. z o.o., Limanowa, Poland). Process control, automation, and data acquisition were performed using a CP6600 controller with an integrated panel PC (Beckhoff Automation GmbH & Co. KG, Verl, Germany).

Prior to the gas flow measurements and gas chromatographic analysis, water vapor present in the cathodic gas stream was condensed in a glass-tube heat exchanger cooled to 0 °C using a CC-K6 circulation thermostat (Peter Huber Kältemaschinenbau SE, Offenburg, Germany). Additional gas purification was achieved using two impingers connected in series, followed by membrane filtration. The first impinger, filled with distilled water, served as a gas-washing unit, whereas the second, containing silica gel, removed residual moisture. Subsequently, MCE gridded membrane filters (Membrane Solutions LLC, Auburn, WA, USA) were used to remove suspended particles prior to gas flow measurements and GC analysis. The anodic gas stream underwent a similar purification procedure, except for the condensation and chromatographic analysis steps.

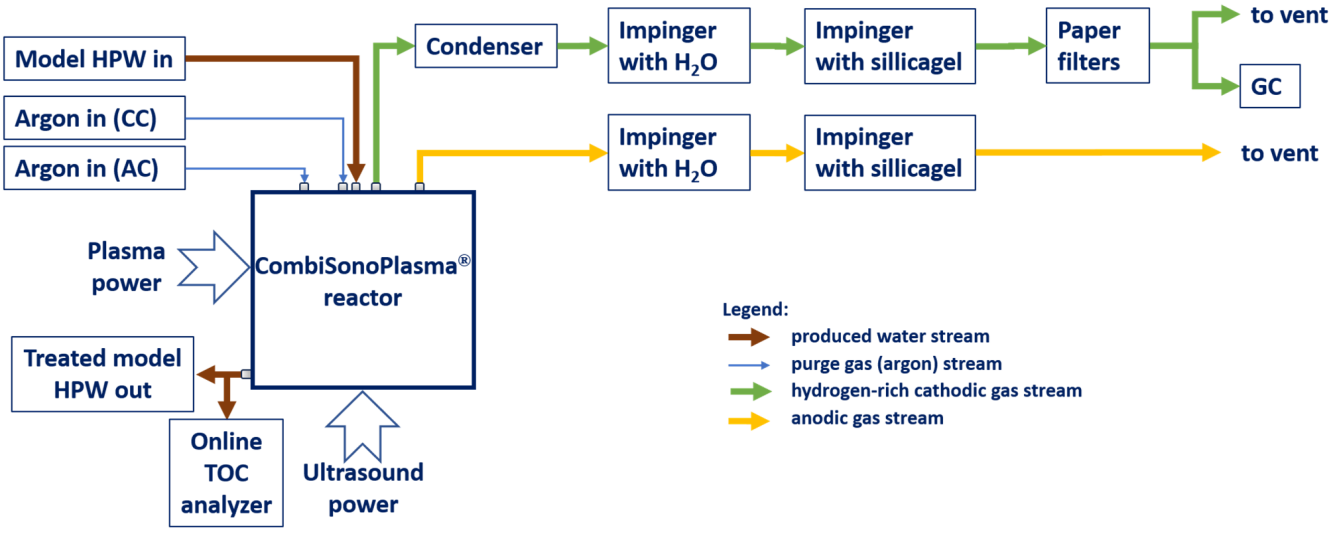


Figure 2. Scheme of the experimental setup [16]: CC, AC and GC denote the cathodic chamber, anodic chamber, and gas chromatograph, respectively.

Argon supply and cathodic outlet gas flow rates were measured using Aalborg rotameters (Aalborg Instruments & Controls, Inc., Orangeburg, NY, USA). The composition of the cathodic gas mixture was determined qualitatively and quantitatively using an 8610C gas chromatograph (SRI Instruments, Inc., Torrance, CA, USA) equipped with a thermal conductivity detector (TCD). The electrode mass loss was determined by weighing the discharge electrode before and after each experimental run using an AS220.3Y analytical balance (RADWAG Wagi Elektroniczne, Radom, Poland).

The performance of the ultrasonic-assisted PDSE reactors (V1, V2, and V3) during 120 min of continuous operation was evaluated based on (i) the prevention of crude oil entrainment from the cathodic compartment, thereby increasing its residence time within the compartment and enhancing its degradation, (ii) formation of gaseous oil decomposition products (CO, CO_2, and CH_4) and TOC reduction as indicators of the degree of crude oil degradation, and (iii) hydrogen generation as a valuable energy co-product.

In all experiments, the immersion depth of the tungsten discharge electrode was maintained at 5 mm using an automatic HPW level control system operating in both the cathodic and anodic compartments. The ultrasonic irradiation amplitude was fixed at 15% of the maximum output of the ultrasonic generator. A constant root mean square (RMS) voltage of 70 V was supplied by the autotransformer between the anode and cathode

throughout the experiments. The distance between the sonotrode tip and the model HPW surface was maintained at 36 mm.

Photographs of the experimental setup and Reactor V1 are provided in [16].

3.2. Safety Measures and Explosion Risk Mitigation

To minimize the risk of explosion, several safety measures were implemented throughout all experiments. The reactor was continuously purged with argon before, during, and after operation, with the inert gas introduced directly into the reactor chambers to prevent the formation of combustible hydrogen–oxygen mixtures. Argon was selected instead of nitrogen because its higher density promotes displacement of air and filling of potential dead volumes, thereby reducing the accumulation of hydrogen and oxygen. Continuous argon dilution maintained the oxygen concentration well below the limiting oxygen concentration (LOC) for hydrogen combustion; the measured oxygen concentration in the product gas was below 1.4 vol%, which is significantly lower than the commonly reported LOC. Additional protection against flame propagation was provided by water impingers (bubblers) and flashback arrestors installed in the gas line. Furthermore, all experiments were conducted under continuous gas flow at near-atmospheric pressure without compression of the produced gases, further reducing the explosion hazard [17–19].

4. Results and Discussion

4.1. Entrainment Effect of the Crude Oil by the Model HPW Flow

Here, we demonstrate the entrainment of crude oil from the cathodic compartment to the anodic compartment by the model HPW flow in reactors V1 and V3, as illustrated in Figure 3.

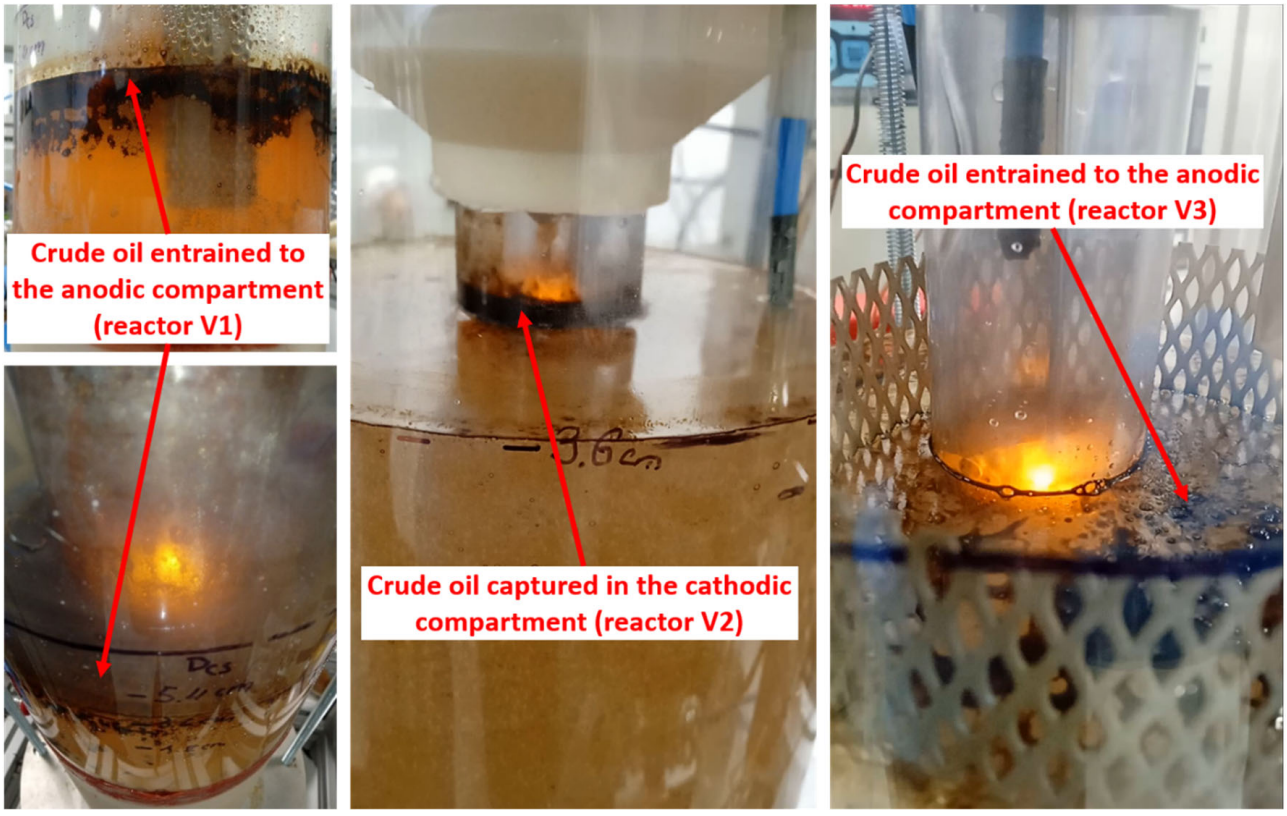


Figure 3. Entrainment of crude oil from the cathodic to anodic compartment observed in reactor V1 (**a**) and reactor V3 (**c**), and crude oil trapping in the cathodic compartment observed in reactor V2 (**b**).

However, as evident from Figure 3, crude oil entrainment from the cathodic compartment to the anodic compartment by the flowing model HPW was substantially greater in reactors V1 (Figure 3a) and V3 (Figure 3c). In contrast, reactor V2 demonstrated a pronounced crude oil retention effect, with no visible accumulation of crude oil observed in the anodic compartment (Figure 3b). This phenomenon is likely associated with the advanced sonotrode arrangement in reactor V2. The deeper penetration of the sonotrode into the cathodic compartment (as shown in Figure 1b), combined with the action of acoustic irradiation, appears to create a hydrodynamic barrier that limits crude oil entrainment from the cathodic compartment to the anodic compartment.

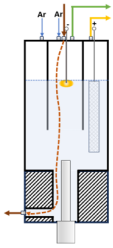
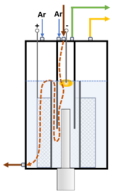
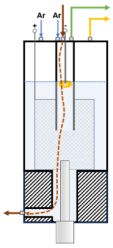
4.2. Performance Comparison of the Reactors V1, V2 and V3

The results obtained in the long-duration experiments on the performance of reactors V1, V2, and V3 are presented in Table 1. Based on these results we found that reactor V2 exhibited the best overall performance in terms of both organic pollutant degradation and hydrogen production. This advantage is attributed to the following:

- The beneficial effect of ultrasonication on PDSE power consumption. As shown in Table 1, the PDSE power consumption in reactor V2 was 33.5% lower than that of reactor V1, and 23.9% lower than that of reactor V3. This reduction is believed to result from the synergistic interaction between ultrasonication and the PDSE process.
- The beneficial effect of PDSE operation on ultrasound power consumption, which was 12.7% lower in reactor V2 than in reactor V1 and 15.1% lower than in reactor V3.
- The energy yield of hydrogen production achieved with reactor V2 was 5.7 L (H_2)/kWh, which was higher than those obtained using reactors V1 and V3. This improvement resulted primarily from the lower total power consumption of reactor V2 (407.2 W), arising from reductions in both PDSE and ultrasound power consumption.
- The average hydrogen-to-oxygen ratio obtained using reactor V2 was 7, which was the highest value among the investigated reactors.
- The detection of all major carbon-containing gaseous products (CO, CO_2, and CH_4) indicates more extensive crude oil decomposition in reactor V2 than in reactors V1 and V3.
- Reactor V2 provided a longer flow path for the HPW through the cathodic and anodic chambers, thereby increasing its residence time.
- Reactor V2 demonstrated an effective crude oil retention effect within the cathodic compartment, preventing crude oil entrainment into the anodic compartment by the model HPW flow. In contrast, noticeable crude oil transfer was observed in reactors V1 and V3, as shown in Figure 3.
- In reactor V2, the relative disintegration rate of the discharge electrode was 0.12 mg/MJ, measured as the weight loss of the discharge electrode [mg] per total energy consumption in the ultrasound-assisted PDSE process [MJ]. This value was significantly lower than the value of 121.48 mg/MJ measured in reactor V1. In reactor V3, the discharge electrode exhibited an increase in weight due to the accumulation of non-removable, electrically non-conductive solid deposits (fouling) on its surface.

It should be noted that the TOC reduction observed for reactor V2 does not fully represent its actual treatment efficiency. The intense ultrasonic irradiation enhances crude oil decomposition while simultaneously promoting the emulsification and fragmentation of oil droplets into low-molecular-weight organic compounds with increased water solubility. Consequently, some fraction of the degradation products remains dissolved in the aqueous phase, leading to a lower measured apparent TOC removal. Therefore, TOC reduction alone may underestimate the actual crude oil degradation performance of reactor V2.

Table 1. Performance of reactors V1, V2, and V3.

Parameter	Configurations of the Reactor		
			
	Reactor V1	**Reactor V2**	**Reactor V3**
PDSE power [W]	337.3	294.6	386.9
Power consumption by the ultrasound generator [W]	169.2	112.6	132.7
Total power consumption [W]	506.5	407.2	519.6
Average flow rate of the gas mixture evolved from the cathodic compartment (argon + gaseous by-products) [smLpm]	524.2	494.9	494.2
Average H_2 concentration in the cathodic gas mixture [vol%]	8.358	7.808	7.153
Average O_2 concentration in the cathodic gas mixture [vol%]	1.387	1.116	1.184
Average CO concentration in the cathodic gas mixture [vol%]	0	0.056	0
Average CH_4 concentration in the cathodic gas mixture [vol%]	0.002	0.024	0.004
Average CO_2 concentration in the cathodic gas mixture [vol%]	0.055	0.256	0.059
Average H_2/O_2 ratio in the cathodic gas mixture	6.028	7.0	6.043
Average electric current [A]	4.01	3.32	4.45
Average voltage measured between anode and cathode [V]	84.6	88.7	87.0
Energy yield of hydrogen production [L(H_2)/kWh]	5.2	5.7	4.1
TOC reduction [%]	65.6	35.2	69
Relative disintegration rate of the discharge electrode [mg/MJ]	121.48	0.12	−0.4 *

Notes: * The observed increase in discharge electrode weight was attributed to non-removable solid deposits formed on its active surface during exposure to the model HPW.

4.3. Synergetic Effect of PDSE on the Reduction in Power Consumption by the Ultrasound Generator

Representative experimental results illustrating this effect are presented in Figure 4.

Based on our previous findings reported in [10] regarding the beneficial effect of indirect sonication on plasma formation and the energy characteristics of cathodic PDSE, a similar enhancement was expected when direct sonication was employed. However, a comparison of the present results obtained using the different reactor configurations (V1, V2 and V3) revealed one unexpected phenomenon: PDSE operation reduced the power consumption of the ultrasound generator.

For reactor V1 (Figure 4a,d,g), the ultrasound generator initially consumed 196.6 W and subsequently stabilized at approximately 174.7 W during the first 5000 s of operation. After activation of the ultrasound generator, the PDSE voltage (blue symbols) gradually increased from 0 V to a level sufficient to sustain plasma formation. During this period, fluctuations in the PDSE voltage and current (orange symbols) were attributed to variations in the model HPW levels within the cathodic and anodic chambers. Once the PDSE voltage stabilized after approximately 5000 s, the average power consumption of the ultrasound

generator decreased to 159.8 W. Consequently, the average ultrasound power consumption throughout the experiment was 169.2 W.

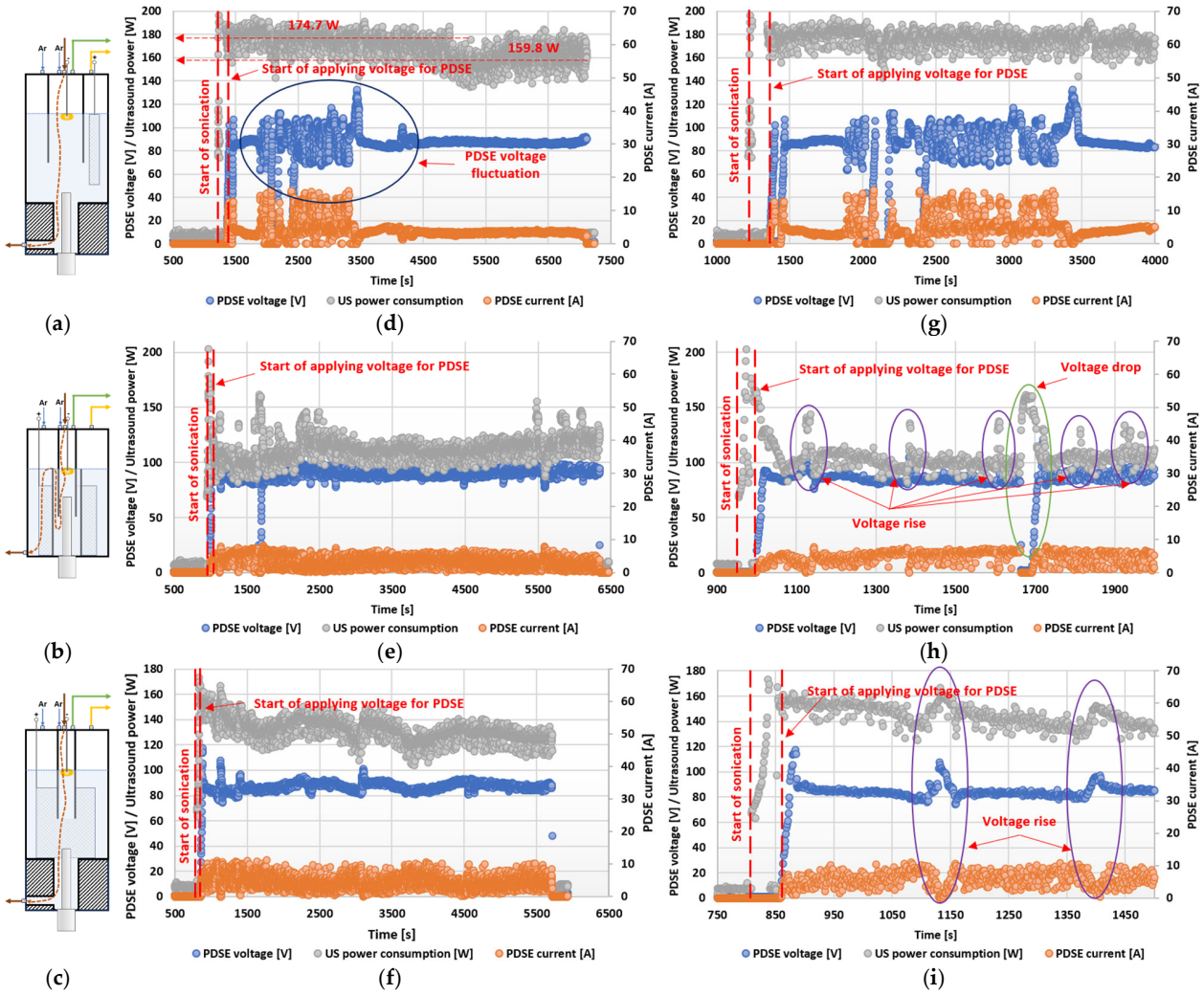


Figure 4. Representative experimental results showing changes in PDSE voltage, PDSE current, and ultrasound (US) power consumption over time: (**a**–**c**) reactor configurations V1, V2, and V3; (**d**–**f**) temporal profiles recorded during the entire experiments with reactors V1, V2, and V3, respectively; and (**g**–**i**) magnified views of the results at the initial experimental periods for reactors V1, V2, and V3, respectively.

Such an effect was much more pronounced for reactor V2 (Figure 4b,e,h). Initially, the ultrasound power consumption increased to 202.9 W and then rapidly decreased to 82.6 W, while the PDSE voltage increased from 0 to 92.9 V, corresponding to a reduction of 59.3%. Thereafter, the power consumption stabilized at approximately 112.6 W. Temporary fluctuations in PDSE voltage during the experiment (at 1135, 1387, 1610, 1813, and 1910 s) resulted in an average increase in ultrasound power consumption of approximately 20%. Furthermore, when the PDSE voltage dropped to 0 V at 1676 s, causing plasma extinction, the ultrasound power consumption increased by approximately 43% relative to its average operating value.

A similar trend in ultrasound power consumption was observed for reactor V3 (Figure 4c,f,i). The ultrasound generator power consumption initially reached 173.3 W and subsequently decreased by 23.4% to an average value of 132.7 W following plasma development. However, transient increases in PDSE voltage were accompanied by corresponding increases in ultrasound generator power consumption. For example, at 1133 s, a

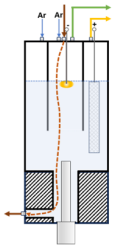
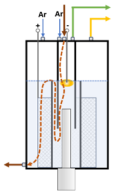
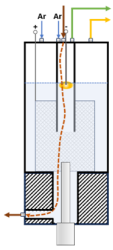
23.9% increase in PDSE voltage resulted in a 25.5% increase in ultrasound generator power consumption, while at 1408 s, a 10.8% increase in PDSE voltage led to a 13.9% increase in ultrasound generator power consumption.

Table 2 summarizes the reduction in ultrasound generator power consumption associated with the transition from conventional DC electrolysis to the PDSE regime.

Because all other operating conditions were maintained constant, the observed reduction in ultrasound power consumption appears to be directly related to the PDSE process itself. Therefore, a new phenomenon is reported, namely a reverse synergistic effect of PDSE on ultrasound energy demand. Although temporary increases in the power consumption of the ultrasound generator were observed during periods of significant PDSE voltage fluctuations, the overall effect was beneficial, as the sustained plasma formation consistently resulted in a reduction in the average power consumption of the ultrasound generator.

A tentative explanation for this phenomenon can be formulated based on the hydrodynamics of the two-phase flow in the confined region surrounding the sonotrode. Previous study [20] demonstrated that, in a high-gradient flow between coaxial cylinders, the transition from single-phase liquid flow to gas–liquid two-phase flow reduces the electrical power required to drive the system. By analogy, plasma formation in the ultrasound-assisted PDSE reactors generates intense gas evolution, transforming the liquid in the cathodic compartment into a gas–liquid mixture. This modifies the flow characteristics and reduces the hydraulic resistance of the model HPW in the cathodic compartment, resulting in a lower load on the sonotrode and, consequently, reduced electrical power consumption by the ultrasound generator.

Table 2. Summary results on the reduction in the power consumption by the ultrasound generator with the formation of the PDSE regime of the DC electrolysis.

Parameter	 **Reactor V1**	 **Reactor V2**	 **Reactor V3**
Power consumption by the ultrasound generator before attaining PDSE regime of electrolysis [W]	196.6	202.9	173.3
Average power consumption by the ultrasound generator throughout the entire experiment [W]	169.2	112.6	132.7
Relative reduction in the power consumption by the ultrasound generator in the experiment [%]	13.9	44.5	23.4

However, this hypothesis does not fully explain the temporary increases in ultrasound generator power consumption observed during periods of elevated PDSE voltage. Furthermore, although the cathodic flow pattern in reactor V2 was annular (Figure 4b), whereas those in reactors V1 (Figure 4a) and V3 (Figure 4c) were not, the reduction in ultrasound generator power consumption was observed in all three reactor configurations. Consequently, additional experimental and theoretical investigations are required to elucidate the mechanisms responsible for this newly observed synergistic phenomenon.

5. Conclusions

Based on the results obtained in this study, the following conclusions can be drawn:

1. Gas chromatographic analysis demonstrated the presence of all three major carbon-containing gaseous products (CO, CH_4, and CO_2) in the cathodic gas stream generated by reactor V2. This finding suggests that crude oil decomposition was more extensive in reactor V2 than in reactors V1 and V3.
2. Reactor V2 exhibited the highest average hydrogen-to-oxygen ratio, reaching a value of 7. In addition, it effectively retained crude oil within the cathodic compartment, preventing oil entrainment into the anodic compartment by the model HPW flow.
3. A beneficial synergistic effect of direct sonication on PDSE energy consumption was observed. The PDSE power consumption of reactor V2 was 33.5% lower than that of reactor V1, and 23.9% lower than that of reactor V3. This reduction is attributed to the favorable interaction between ultrasonic cavitation and plasma formation, although further research is required to clarify the underlying mechanisms.
4. A reverse synergistic effect of PDSE on ultrasound power consumption was observed for the first time. The most pronounced reduction, amounting to 44.5%, was observed in reactor V2. A tentative explanation for this phenomenon is that the transition of the model HPW to a two-phase flow within the confined space between the sonotrode and the cylindrical baffle separating the anodic and cathodic compartments alters the flow behavior and reduces the hydraulic resistance in the cathodic compartment, thereby decreasing the load on the sonotrode and consequently reducing the electrical power consumption of the ultrasound generator. Nevertheless, additional studies are required to validate this hypothesis and establish the governing mechanisms.
5. The relative disintegration rate of the discharge electrode in reactor V2 was significantly lower than that in reactor V1. Furthermore, unlike reactor V3, no non-removable, electrically non-conductive solid deposits were observed on the discharge electrode surface in reactor V2.
6. Considering crude oil decomposition, hydrogen production, the hydrogen-to-oxygen ratio, crude oil retention capability, overall energy performance and the low relative disintegration rate of the discharge electrode, reactor V2 demonstrated the most favorable operating characteristics among the investigated reactor configurations.

6. Patent and Trademark

The reactor design is the subject of a patent application No. P.451120 [WIPO ST 10/C PL451120], filed in 2025.

CombiSonoPlasma® is a registered trademark of the Research and Innovation Centre Pro-Akademia (Konstantynów Łódzki, Poland).

Author Contributions: Conceptualization, S.B., M.S. and N.M.A.M.; methodology, S.B., O.H., J.M. (Justyna Markiewicz), N.M.A.M. and M.S.; formal analysis, S.B. and O.H.; investigation, S.B., J.M. (Justyna Markiewicz), M.S.; resources, J.M. (Justyna Markiewicz) and M.S.; data curation, S.B.; writing—original draft preparation, S.B. and O.H.; writing—review and editing, J.M. (Jerzy Mizeraczyk); visualization, S.B., O.H. and M.S.; supervision, M.S. and J.M. (Jerzy Mizeraczyk); project administration, M.S.; funding acquisition, S.B. and M.S. All authors have read and agreed to the published version of the manuscript.

Funding: This work was performed as part of the WASTE4H2 project financed by the Polish National Centre for Research and Development (Polish: NCBR) under the INNOGLOBO program (the grant agreement no. INNOGLOBO/I/77/WASTE4H2/2022).

Data Availability Statement: The raw data supporting the conclusions of this article will be made available by the authors on request.

Conflicts of Interest: The authors declare no conflicts of interest.

References

1. Gupta, S.K. Contact Glow Discharge Electrolysis: A Novel Tool for Manifold Applications. *Plasma Chem. Plasma Process.* **2017**, *37*, 897–945. [CrossRef]
2. Nurcahya, M.; Sijabat, T.D.; Liuvinia, T.; Saksono, N. Study of stainless steel and tungsten performance as plasma electrode materials and u-pipe air injector for the degradation of Remazol Red using the air injection plasma electrolysis method. *Int. J. Plasma Environ. Sci. Technol.* **2025**, *19*, e01004. [CrossRef]
3. Rottach, K.; Lang, G.H.; Gastaldi, M.; Gerbaldi, C.; Bonomo, M. On the impact of electrolyte temperature on contact glow discharge electrolysis. *Electrochem. Commun.* **2023**, *153*, 107542. [CrossRef]
4. Jamil, T. Role of Advance Oxidation Processes (AOPs) in Textile Wastewater Treatment: A Critical Review. *Desalin. Water Treat.* **2024**, *318*, 100387. [CrossRef]
5. Lin, L.; Sun, Z.; Chen, H.; Zhao, L.; Sun, M.; Yang, Y.; Liao, Z.; Wu, X.; Li, X.; Tang, C. Recent Advances in Electrocatalytic Two-Electron Water Oxidation for Green H_2O_2 Production. *Acta Phys. Chim. Sin.* **2024**, *40*, 2305019. [CrossRef]
6. Bespalko, S.; Mizeraczyk, J. Overview of the Hydrogen Production by Plasma-Driven Solution Electrolysis. *Energies* **2022**, *15*, 7508. [CrossRef]
7. Phull, S.S.; Newman, A.P.; Lorimer, J.P.; Pollet, B.G.; Mason, T.J. The development and evaluation of ultrasound in the biocidal treatment of water. *Ultrason. Sonochem.* **1997**, *4*, 157–164. [CrossRef] [PubMed]
8. Kerboua, K.; Hamdaoui, O.; Islam, M.H.; Alghyamah, A.A.; Hansen, H.E.; Pollet, B.G. Low carbon ultrasonic production of alternate fuel: Operational and mechanistic concerns of the sonochemical process of hydrogen generation under various scenarios. *Int. J. Hydrogen Energy* **2021**, *46*, 26770–26787. [CrossRef]
9. Rashwan, S.S.; Dincer, I.; Mohany, A.; Pollet, B.G. The Sono-Hydro-Gen process (Ultrasound induced hydrogen production): Challenges and opportunities. *Int. J. Hydrogen Energy* **2019**, *44*, 14500–14526. [CrossRef]
10. Bespalko, S.; Siedlecki, M.; Markiewicz, J.; Mizeraczyk, J. Effect of the indirect sonication on the plasma formation and energy parameters in the cathodic regime of the plasma-driven solution electrolysis. *Przegląd Elektrotech.* **2024**, *10*, 277–280. [CrossRef]
11. Merouani, S.; Dehane, A.; Hamdaoui, O. A review on the integration of ultrasonication in hybrid systems for enhanced hydrogen yield. *Ultrason. Sonochem.* **2025**, *121*, 107552. [CrossRef] [PubMed]
12. Zeng, C.; Teoh, Y.H.; How, H.G.; Idroas, M.Y.; Le, T.D. Ultrasound-enhanced water electrolysis for hydrogen production: Mechanisms, metrology and energy metrics. *J. Electrochem. Sci. Eng.* **2026**, *16*, 3045. [CrossRef]
13. Pournemati, K.; Habibi-Yangjeh, A.; Salmanzadeh-Jamadi, Z. A critical review on application of emerging hybrid cavitation–plasma technology for remediation of wastewater effluents. *J. Water Process Eng.* **2024**, *67*, 106183. [CrossRef]
14. Saad, A.; Bai, L.; Christensen, F.M.; Luo, S.; Bentien, A.; Ashokkumar, M.; Wei, Z. Ultrasound-enhanced Alkaline Water Splitting with Fast Bubble Release and Sustained Ni Catalysts. *Appl. Catal. B Environ. Energy* **2025**, *367*, 125079. [CrossRef]
15. Merouani, S.; Dehane, A.; Hamdaoui, O. Hydrogen production via water ultrasonication: A review. *Ultrason. Sonochem.* **2025**, *120*, 107515. [CrossRef] [PubMed]
16. Bespalko, S.; Al Mhanna, N.; Markiewicz, J.; Majzer, R.; Halychyi, O.; Al-Jabri, N.; Said Alazry, M.; Siedlecki, M. CombiSonoPlasma® Process for Efficient Degradation of Organic Pollutants in Hypersaline Produced Water with Concurrent Hydrogen Production. *Int. J. Plasma Environ. Sci. Technol.* 2026; *accepted*.
17. Reinhardt, H.-J.; Himmen, H.R.; Kaltenegger, J. *Inerting in the Chemical Industry*; Linde AG: Pullach, Germany, 2015.
18. European Hydrogen Safety Panel. *EHSP Guidance on Hydrogen Safety Engineering—Guidance Document; Clean Hydrogen Joint Undertaking*; Clean Hydrogen Partnership: Brussels, Belgium, 2023.
19. European Industrial Gases Association. *Standard Procedures for Hydrogen Supply Systems (EIGA Doc. 250/24)*; European Industrial Gases Association: Brussels, Belgium, 2024.
20. Bespalko, S.; Halychyi, O.; Yovchenko, A.; Plakhotnyi, O.; Poliakov, S.; Kaleinikov, G.; Roha, M.; Fenko, I. Experimental testing of the heating performance of a rotor-type dissipative liquid heater. *Int. J. Energy Environ. Eng.* **2021**, *12*, 39–54. [CrossRef]

Disclaimer/Publisher's Note: The statements, opinions and data contained in all publications are solely those of the individual author(s) and contributor(s) and not of MDPI and/or the editor(s). MDPI and/or the editor(s) disclaim responsibility for any injury to people or property resulting from any ideas, methods, instructions or products referred to in the content.